

## LIGHT TO MASS VARIATIONS WITH ENVIRONMENT

R. BRENT TULLY

Institute for Astronomy, University of Hawaii, Honolulu, HI 96822

Version: 2004, September 9

### ABSTRACT

Large and well defined variations exist between the distribution of mass and the light of stars on extragalactic scales. Mass concentrations in the range  $10^{12} - 10^{13} M_{\odot}$  manifest the most light per unit mass. Group halos in this range are typically the hosts of spiral and irregular galaxies with ongoing star formation. On average  $M/L_B \sim 90 M_{\odot}/L_{\odot}$  in these groups. More massive halos have less light per unit mass. Within a given mass range, halos that are dynamically old as measured by crossing times and galaxy morphologies have distinctly less light per unit mass. At the other end of the mass spectrum, below  $10^{12} M_{\odot}$ , there is a cutoff in the manifestation of light. Group halos in the range  $10^{11} - 10^{12} M_{\odot}$  can host dwarf galaxies but with such low luminosities that  $M/L_B$  values can range from several hundred to several thousand. It is suspected that there must be completely dark halos at lower masses. Given the form of the halo mass function, it is the low relative luminosities of the high mass halos that has the greatest cosmological implications. Of order half the clustered mass may reside in halos with greater than  $10^{14} M_{\odot}$ . By contrast, only 5 – 10% of clustered mass would lie in entities with less than  $10^{12} M_{\odot}$ .

*Subject headings:* dark matter — galaxies: clusters — galaxies: dwarf — galaxies: luminosity function, mass function

### 1. INTRODUCTION

It would be remarkable if the naive assumption that light linearly traces mass is correct. Indeed, on scales of tens of kiloparsecs around galaxies it is known from rotation curve information that dark matter is more dispersed than starlight. It has long been entertained that dark matter might be more dispersed than light on megaparsec scales (Kaiser 1984). If so, we would say there is a ‘bias’ between what we see and the physically more fundamental parameter, the mass. Semi-analytic models (Blanton et al. 1999; Somerville et al. 2001; Ostriker et al. 2003) anticipate variations in the conversion of baryons into stars and the manifestation as starlight at both very low and very high densities.

Theoretical considerations prepare us for the possibility of a complex relationship between the distribution of mass and of the lighthouses sitting atop that mass. In this article we present observational evidence for such complexity. Three environmental regimes will be considered. At home in the Local Group we find ourselves in an intermediate regime, common to the majority of spiral galaxies. Most elliptical galaxies find themselves in a high density regime. Then there is a low density regime where galaxies are few or absent. What is the relationship between light and mass in each of these three kinds of environments?

### 2. GROUPS OF GALAXIES

Visible galaxies are embedded in halos that extend beyond the radii of observable gas and stars. We need to go to the scale of groups and clusters to obtain a measure of the total mass of galaxies. The current investigation relies on the analysis of groups by Tully (1987); hereafter T87. The individual galaxies associated with the groups in T87 are identified in Table II of Tully (1988). This particular group compendium has the attractive features that (a) it was constructed with quantitative, well defined

rules, (b) the groups have been demonstrated to contain few interlopers, and (c) a subset has a high level of volume completeness.

The group catalog was constructed through a tree or ‘dendrogram’ procedure. The construction begins by looking for the linkage between galaxies that gives the largest value of the product  $L_B/R_{ij}^2$  where two candidates  $i$  and  $j$  are considered from the ensemble of  $N$  objects,  $L_B$  is the blue luminosity of the brighter candidate, and  $R_{ij}$  is the linear separation between the two. For details on the calculation of  $R_{ij}$  from angular and radial velocity information see T87 but essentially, for linkages relevant to group scales, the  $R_{ij}$  are based on angular separations only. The dominant pair that is selected is now inserted back into the catalog as a single unit with the sum of the component luminosities and with position and velocity constructed from the luminosity weighted contributions of the components. There are now  $N - 1$  objects to consider and the process is repeated, over and over, until  $N = 1$ .

In a dendrogram constructed in this manner, ultimately all galaxies under consideration are linked. Obviously there is a transition at some point from collections of galaxies that are bound to those that are unbound. The issue of how to distinguish the bound and unbound domains was the subject of extensive discussion in T87. A crossing time argument was used. At any point in the dendrogram, the galaxies that are linked together can be characterized by a separation dimension, the inertial radius  $R_I$ , and a velocity dispersion,  $V_p$ . The crossing time  $t_x \sim R_I/V_p$  (see T87 for details including corrections for projection) can be compared with the free expansion timescale, the inverse of the Hubble Constant,  $H_0$ . Units with  $t_x H_0 \ll 1$  have a high probability of being bound. Units with  $t_x H_0 > 1$  can be inferred to be unbound. With a judicious choice of level, the dendrogram could be split between mostly bound and mostly unbound. It would follow from this choice, allowing for measurement and projection errors, that es-

essentially all the merged units that make the dendrogram cut on the high density side would have  $t_x H_0 < 1$ .

An interesting aspect of this analysis is that it provides an inventory not only of all the galaxies in a volume that are in groups but also *all that are not* in groups. In the sample considered by T87 there was the usual incompleteness with distance. However a high Galactic latitude volume with the distance limit of  $25h_{75}^{-1}$  Mpc ( $h_{75} = H_0/75$ ) has completion in the sense that all galaxies brighter than  $M_B^*$  are included. Within this volume, T87 identified 179 groups of 2 or more galaxies and 49 groups of 5 or more. For statistical robustness, we will restrict most of the following discussion to the groups of 5 or more galaxies (one of the small groups in T87 has been boosted to above 5 members with our current inventory, giving us 50 groups to consider).

We should note a subtle point that arises because the dendrogram linkages involve luminosities. Linkages that involve bright galaxies are made more easily, as might well be reasonable if brighter galaxies are more massive. However could we miss linkages in cases where mass is under-represented by light? This possibility would potentially undermine the basis of this investigation. It is to be noted that T87 provides a safety net to guard against this concern. In addition to the dendrogram cut that resulted in the definition of ‘groups’, a second cut was made an order of magnitude lower in luminosity density that resulted in what were called ‘associations’. We will first continue with a discussion of the groups but later we will revisit the entities called associations.

### 3. LIGHT TO MASS VARIATIONS WITHIN GROUPS

The analysis in T87 missed an amazing correlation! It is seen in Figure 1, which draws on data extracted from T87 and presented here in Table 1. The data in the left panel represent all the 50 groups in the volume with completion above  $M_B^*$ . In the right panel, symbols distinguish between groups with majority early morphological types (E-S0-Sa: filled squares) and groups with majority late types (Sab-Irr: open circles). There are fewer points in this panel because, in order to make a statistically meaningful distinction in morphological class, we require there be at least 6 galaxies brighter than  $M_B = -17$ . These groups are distinguished by an entry in the third column of Table 1 where the percentage type Sa or earlier among galaxies brighter than  $M_B = -17$  is given. The numbers of early type groups are small in this restricted local volume, so the slightly more distant early type groups Virgo W, Antlia, and NGC 5846 are also considered (last 3 entries in Table 1).

Groups with crossing times much less than a Hubble time have relatively high mass to light ( $M/L_B$ ) ratios, values of several hundred in solar units (masses from T87 are unweighted virial masses following the definition given in Section 6 of this paper). Groups with crossing times that approach a Hubble time have  $M/L_B$  ratios that are much more modest, a few tens in solar units. It is also seen that there is a strong correlation between crossing time and the morphological classification. If the sample is split at a crossing time as a fraction of the Hubble timescale of  $0.2H_0$  then almost all the groups with shorter crossing times are dominated by early types (8 of 9) and almost all

the groups with longer crossing times are dominated by late types (11 of 14).

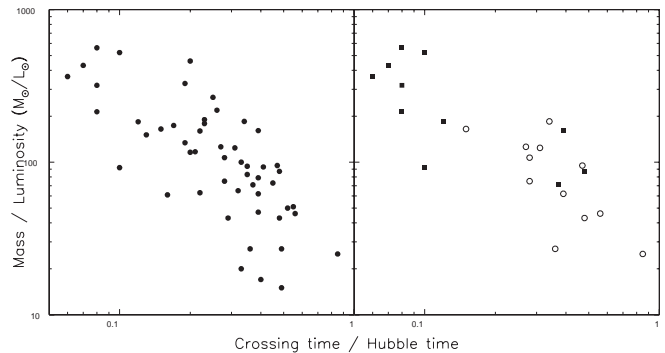


FIG. 1.— Correlation between mass/light ratio and group crossing time. *Left panel:* all groups with 5 or more members in the volume limited T87 sample. *Right panel:* Subset of groups with at least 6 members with  $M_B < -17$  distinguished according to whether a majority of galaxies in the group are E-S0-Sa (filled squares) or Sab-Sc-Irr (open circles).

Could the correlation seen in Fig. 1 be induced by parameter coupling? The vertical axis has dependencies on  $V_p^2 R$  while the horizontal axis has dependencies  $R/V_p$ , where  $R$  is a characteristic of the group dimension and  $V_p$  is the velocity dispersion. Changes in  $V_p$  cause shifts in the sense of the observed correlation. Changes in  $R$  cause shifts orthogonal to the correlation. The concern would have to be with  $V_p$  values but the typical measurement uncertainties in these values are 20% for the groups in question, much smaller than the factor ten range in crossing time values. Most clearly, though, the correlation cannot be an artifact of parameter errors and coupling between the axes because there is a strong correlation between the parameter of either axis in Fig. 1 and the morphology of the galaxies. The qualitative morphological information is decoupled from the measured parameters. In the right panel of Fig. 1, the early type groups have a median crossing time about a factor 3 less and a median  $M/L_B$  about a factor of 3 higher than the late type groups.

Could the correlation be an artifact caused by systematic departures from virial equilibrium? Presumably the groups with the shortest crossing times have most closely approached the virial equipartition of energy. There could be a systematic mis-estimation of mass with the virial approximation that depends on the dynamical age of a system. Pacheco (private communication) has studied the collapse of a group with the expression:

$$\frac{1}{2} \frac{d^2 I}{dt^2} = 2(T + U) + W \quad (1)$$

where  $I$  is the moment of inertia of the system,  $T$  is the kinetic energy in the randomized motions of the constituents,  $U$  is the kinetic energy in the ordered motions of infall, and  $W$  is the potential energy. Pacheco made analytic assumptions about what happens when, during the collapse, violent relaxation (Lynden-Bell 1967; Funato et al. 1992) causes the transform of energy from bulk motion to a state approximated by the virial condition. Dynamical friction induces the transfer of energy from ordered to random motions. The approach to equilibrium, with  $d^2 I/dt^2 \sim 0$ , occurs on the order of one dynamical timescale ( $t_{dyn} = (G\rho)^{-1/2} \sim t_x$  where  $\rho$  is the average

density of the group within the virial radius). Measurements of groups caught before relaxation would tend to result in underestimates of mass by typically 20% and a factor 2 in the extreme (theoretically assuming full 3-D information is available).

The situation is complex. It was suggested by Barnes (1985) that virial mass estimates might be biased low because of segregation as the visible components sink toward the center relative to dark matter. This possible systematic would increase as the group ages, consequently it would run counter to the correlation seen in Fig. 1. There is room for further analysis of the properties of groups extracted from cosmological simulations. High resolution is required to avoid the concern of artificial 2-body relaxation from massive numerical particles.

There is firmer ground on the observational side. There is general agreement that groups and clusters with high densities and short dynamical times have  $M/L_B$  values of several hundred. These circumstances are confirmed by X-ray and gravitational lensing studies. We suggest that the trend to substantially lower  $M/L_B$  values for systems with longer dynamical times seen in Fig. 1 is consistent with what is now known from the few detailed studies of low density groups.

The situation is clearest in the Local Group and has received confirmation from recent studies of the nearest neighboring groups. These groups are represented in the left panel of Fig. 1 but are not sufficiently populated to enter the right panel. They lie in the lower right corner, with large crossing times and low  $M/L_B$ .

The Local Group encompasses two dynamical regimes. On a 100 kpc scale, each of the two major galaxies host a school of minor systems that approximate virial conditions. On a 1 Mpc scale, the two major galaxies and ten or so other small galaxies are falling together, most on first approach. This latter assertion is based on the observation that almost all the Local Group systems that are not tightly associated with either of the two major galaxies have negative velocities in the Local Group standard of rest (NGC 6822 is an exception).

The masses of the Milky Way and Andromeda sub-groups can be estimated through the virial theorem since these sub-systems have densities and crossing times that suggest they are dynamically evolved (Evans et al. 2000). The stellar stream on a scale of 125 kpc around M31 provides a compatible mass estimate (Ibata et al. 2004). Each sub-group is determined to have  $0.7 - 1 \times 10^{12} M_\odot$ . The mass of the larger infall region can be estimated separately. One approach follows the Kahn-Woltjer (1959) timing argument. A variation on this approach is provided by the identification of the current turnaround radius or zero-velocity surface for the Local Group (Sandage 1986; Karachentsev et al. 2002c). There is the important result that the sum of the masses of the Andromeda and Milky Way sub-systems add to approximately the mass determined to lie within the zero-velocity surface of  $1.2 \times 10^{12} M_\odot$ . A similar mass is found from orbit reconstructions (Peebles 1995). Our naive virial estimation (Table 1: group 14-12) gives a Local Group mass of  $1 \times 10^{12} M_\odot$  and  $M/L_B = 17 M_\odot/L_\odot$ , in factor 2 agreement with other results.

Recent observations of the resolved stars in nearby

galaxies with Hubble Space Telescope have dramatically improved our knowledge of distances to many nearby galaxies and hence of the structure of the nearest groups. We now know that the best studied neighboring groups, those about M81 (Table 1: group 14-10) and Centaurus A (Table 1: group 14-15), have dumbbell structures like the Local Group. In both cases the two largest galaxies are surrounded by swarms of small galaxies which transit their hosts in times much less than the age of the universe. Almost certainly in the case of the M81 Group and plausibly in the case of the Centaurus Group, the substructures are falling together. As with the Local Group, the masses inferred for the entire bound entities (2 and 3 times  $10^{12} M_\odot$  respectively) are close to the sum of the masses of the dynamically evolved subcomponents (Karachentsev et al. 2002a,b). The halos of the giant galaxies must not extend much beyond the domain of the immediate companions and the group  $M/L_B$  values are a few tens. These groups that are overall spiral rich and low density evidently have  $M/L_B$  values well below 100. The virial approximation for these groups, while crude, gives mass estimates that are not strongly deviant.

While theoretical expectations might cause one to anticipate systematic underestimations of mass assuming the virial approximation, studies of the nearest structures reveal that a crude application of the virial theorem may frequently result in *overestimations* of mass. Frequently, unbound objects will be erroneously included as group members. The availability of good distances to individual galaxies shows that the very nearby Sculptor Group (Table 1: 14-13) and CVn I Group (Table 1: 14-07) are composites of regions that are unlikely to be bound in the ensemble. The inclusion of expansion velocities and the inflation of group scale cause overestimates of mass. These effects are pernicious for the extended, low dispersion systems that inhabit the lower right corner of Fig. 1.

The limited information available on morphological variations from studies of nearby groups is giving a hint of higher mass in early type systems. The kinematics of the sub-group around Centaurus A suggest a mass of  $4 \times 10^{12} M_\odot$  and  $M/L_B \sim 100 M_\odot/L_\odot$  (albeit including the large spiral NGC 4945) while the M83 sub-group is found to have a mass of  $1 \times 10^{12} M_\odot$  and  $M/L_B \sim 50 M_\odot/L_\odot$ . The elliptical Cen A may have a higher  $M/L_B$  by a factor 2-3 relative to the large spirals in our vicinity. The situation in the nearest groups is reviewed by Karachentsev (2004).

Figure 2 shows the correlation between mass and light for the TF87 sample of nearby groups. In the left panel, all the 50 groups in the volume-limited sample with at least 5 members are represented. The groups with  $t_x H_0 < 0.2$  are plotted with filled squares and the groups with larger crossing times are plotted with open circles. The 3 more distant early type groups, all with  $t_x H_0 < 0.2$ , are plotted as inverted triangles. The solid line at  $45^\circ$  indicates the mean  $M/L_B$  value determined by T87 for this sample. Again we see that the groups with short crossing times have less blue luminosity per unit of mass. In addition, it can be said that groups with more mass manifest less blue light per unit mass.

We consider the same data in the right panel but now the differentiation is made on the basis of the morphology

of the groups. It is seen again that the qualitative morphological description and the quantitative crossing time measure provide an equivalent basis for distinguishing between high and low  $M/L_B$  systems.

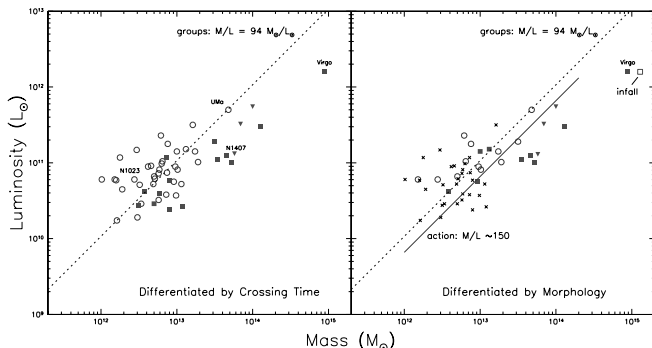


FIG. 2.— Correlation of mass and blue luminosity. *Left panel:* Groups with  $t_{\times}H_0 < 0.2$  are indicated by filled squares and inverted triangles and groups with longer crossing times are indicated by open circles. The mean  $M/L_B$  value of  $94M_{\odot}/L_{\odot}$  for T87 groups is shown by the  $45^{\circ}$  dotted line. The 4 representative groups that are identified (Virgo, Ursa Major, NGC 1023, NGC 1407) are discussed in the text. The 3 inverted triangles represent groups at larger distance than the complete sample. *Right panel:* Same data points but now majority E-S0-Sa groups are indicated by filled squares and inverted triangles and majority Sab-Sc-Irr groups are indicated by open circles. Groups too sparse to be differentiated by morphology are indicated by crosses. This figure shows the  $M/L_B = 94M_{\odot}/L_{\odot}$  dotted line and, in addition, shows the mean result for the field that comes from Numerical Action models, the  $M/L_B = 150M_{\odot}/L_{\odot}$  line. Also, the mass of the Virgo Cluster given by infall constraints in the Numerical Action models is illustrated by the position of the open square.

The Virgo Cluster (group 11-1 in TF87) and three other specific groups are identified in the left panel of Fig. 2. It is instructive to consider the pairwise properties of these groups. It can be seen that the NGC 1407 (51-8) Group has roughly the same mass as the Ursa Major Cluster (group 12-1) but much lower luminosity. The NGC 1407 Group has the same luminosity as the NGC 1023 (17-1) Group but much more mass. These similarities and differences are not in observational doubt. There is a summary of the properties of these groups in Table 1 of Trentham and Tully (2002); see also Fig. 1 in that reference for histograms of the group velocities. The unusual nature of the NGC 1407 Group has been noted by Gould (1993) and Quintana, Fouqué, and Way (1994). The group contains only two  $L^*$  galaxies but has a velocity dispersion of  $385 \text{ km s}^{-1}$ . The Ursa Major Cluster, by contrast, has almost enough luminous galaxies to qualify as an Abell richness class 0 cluster! The velocity dispersion, though, is only  $148 \text{ km s}^{-1}$ . The virial masses of the two groups are almost the same. In the NGC 1407 Group motions are large in a small volume while in the Ursa Major Cluster motions are low in a large volume. Yet the luminosities differ by a factor 5 and  $M/L_B$  values differ accordingly. The NGC 1023 Group is a scaled down version of the Ursa Major Cluster. There are three  $L^*$  galaxies and the group velocity dispersion is only  $57 \text{ km s}^{-1}$ . The NGC 1023 and NGC 1407 groups have similar galaxy content in terms of numbers and luminosity (the type content is late and early, respectively). However the motions in the NGC 1407 Group are a factor of 7 higher. This difference can not be questioned observationally, and the implied mass of the NGC 1407

Group is higher by a factor 30.

In summary of this section, evidence is provided of an order of magnitude variation of  $M/L_B$  that depends on mass and/or stage of dynamical evolution. The derivation of mass from the virial theorem might have biases but there are effects that both raise and lower estimates. The cases that are particularly well studied provide confirmation of the trends shown in Figs. 1 and 2.

#### 4. NUMERICAL ACTION MODELS OF LARGE SCALE FLOWS

There is a strong inference from Numerical Action orbit reconstructions that the Virgo Cluster is very underluminous for its mass compared with the general field. From a first analysis of the Local Supercluster (Shaya, Peebles, and Tully 1995) with 300 distance estimates as constraints and a later analysis (Tully and Shaya 1998) with 900 distance estimates, it was determined that the mean density of the Universe is  $\Omega_m \sim 0.2$ , consistent with an overall mean  $M/L_B \sim 200M_{\odot}/L_{\odot}$  assignment. However, as emphasized in the latter paper, it is not possible with a *single* assignment of  $M/L_B$  for all galaxies to obtain a satisfactory model that simultaneously gives a good description of flows in the general vicinity of the Local Supercluster and a good description of the infall region around the Virgo Cluster.

Evidence for this claim is provided in Figures 3 and 4. The first of these figures show velocity-distance data for galaxies in a group along a specific line-of-sight with respect to the Virgo Cluster. The two panels illustrate attempts to fit this data with two distinct Numerical Action models. The solid curves represent the run of velocity with distance expected by the separate models. In the left panel, a value  $M/L_B = 200M_{\odot}/L_{\odot}$  is assigned to all groups and galaxies. The location of the galaxy data points in velocity and distance cannot be understood in the context of the model in this panel. In the right panel,  $M/L_B = 1000M_{\odot}/L_{\odot}$  is assigned to the Virgo Cluster, and incidentally to all E/S0 knots. In compensation for this increase in the mass of some of the objects,  $M/L_B = 150M_{\odot}/L_{\odot}$  is given all the rest. Now the infall motions toward Virgo are greatly enhanced and the model gives a physical basis for the location of this particular group in velocity-distance space. We see that the group must be slightly nearer than the cluster and falling away from us into the cluster.

The swing in amplitude of the wave in velocity-distance seen in Fig. 3 (the ‘triple-value’ characteristic (Tonry and Davis 1981)) depends on the mass assigned to the cluster. It can be seen that the curve in the right panel of Fig. 3 only minimally reaches the location of the data points, hence represents a *minimum* required mass. A larger mass would cause a larger swing and would not be in conflict with the data but is not required. Fig. 4 shows the constraints provided by many lines-of-sight through the Virgo infall region. The individual points record velocity and angular distance from Virgo, as open circles for galaxies in the cluster proper (defined by the ‘caustic’ radius established by galaxies that have fallen into the cluster and back out to a second turnaround), and as filled circles for galaxies identified to be within the first infall region. To keep the plot clean, galaxies at foreground and background ‘triple-value’ locations have been rejected

based on distance information. The swings in amplitude of the triple-value waves along various lines-of-sight are indicated by the brackets in the two panels. It is clear that the swing generated by the Numerical Action model of the left panel, with  $M/L_B = 200M_\odot/L_\odot$  for all points, fails by a wide margin to explain the infall motions into the Virgo Cluster. The model used in the right panel, with  $M/L_B = 1000M_\odot/L_\odot$  given to the Virgo Cluster and  $M/L_B = 150M_\odot/L_\odot$  assigned to the field, provides a satisfactory description to the observed data.

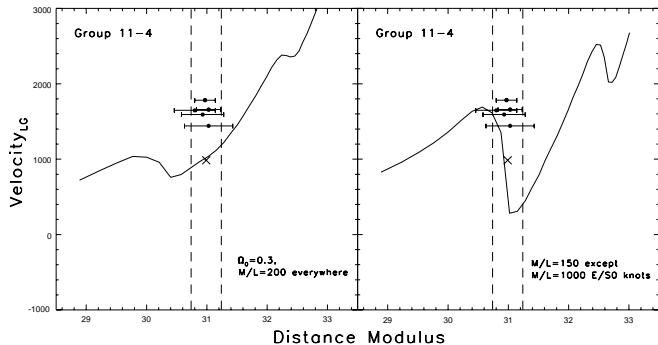


FIG. 3.— Example of model velocities along a line-of-sight close to the direction of the Virgo Cluster. In this case, the line-of-sight is through Group 11-4 in the catalog of Tully (1988). The points with errors correspond to galaxies in this group with distance determinations. The vertical dashed lines bracket the distance of the Virgo Cluster, centered in distance and velocity at the large cross. *Left panel:*  $M/L_B = 200$  for all entries. *Right panel:*  $M/L_B = 1000$  for Virgo and other E/S0 knots, otherwise  $M/L_B = 150$ . The curves are locii of velocities allowed by the models as a function of distance in the specified line-of-sight. The second wave in the velocity curve beyond Virgo occurs because the line-of-sight passes near another E/S0 knot, the Virgo W Cluster, Group 11-24.

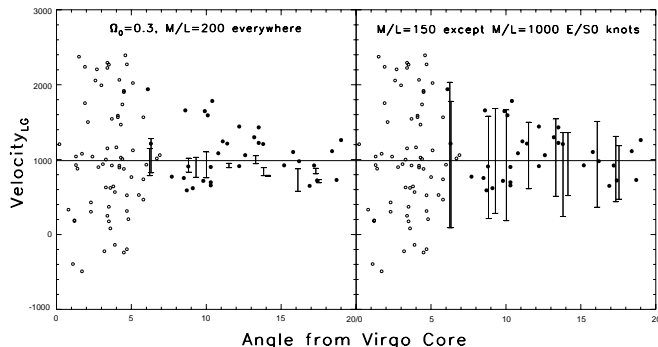


FIG. 4.— Virgo infall constraints from two Numerical Action models. Data points indicate the velocities and separations from the center of the Virgo Cluster of individual galaxies. Galaxies within the  $6^\circ$  caustic of the cluster are indicated by open circles. Galaxies outside the caustic but identified with the infall region are indicated by filled circles. The vertical brackets are located at angles from the center of the cluster that intersect infalling groups, so at lines-of-sight that have received attention in the Numerical Action models. The amplitudes of the brackets illustrate the range of infall velocities anticipated by the two models under consideration. *Left panel:*  $M/L_B = 200$  assigned to all units. *Right panel:*  $M/L_B = 1000$  assigned to Virgo Cluster and other E/S0 knots and  $M/L_B = 150$  otherwise.

Almost a factor 7 higher  $M/L_B$  value is required for the Virgo Cluster than for the general field. The evidence for a lot of mass in the cluster which comes from the extended nature of the infall region (extending to  $\sim 25^\circ$  from the center of the cluster or 8 Mpc) and high infall ve-

locities (galaxies hit the caustic surface of the cluster at  $6^\circ$  with a velocity of  $1500 \text{ km s}^{-1}$ ) requires a remarkable  $1.3 \times 10^{15} M_\odot$  within the 2 Mpc caustic surface of second turnaround. This mass is almost twice the virial mass estimate but it pertains to a radius three times larger than the virial radius. The infall mass estimate pertains to the cluster on its largest scale. It can be noted that a similar conclusion was reached much earlier (Tully and Shaya 1984) with a non-linear but spherically symmetric analytic model of Virgo Cluster infall. The very same conclusions were reached that there had to be a lot of mass for the amount of light in the cluster but much less mass with respect to light in the supercluster environs surrounding the cluster.

The preferred model in the Tully and Shaya (1998) analysis used two discrete  $M/L_B$  assignments:  $M/L_B = 1000M_\odot/L_\odot$  was assigned to 12 E-S0 dominated groups including the Virgo Cluster and  $M/L_B = 150M_\odot/L_\odot$  was assigned otherwise. (The action models do not provide constraints on the masses of the E-S0 groups smaller than Virgo because the triple value regions are too restricted to map infall. The large  $M/L_B$  assignments for these groups were based on the virial information discussed earlier.) It was concluded that  $\Omega_m \sim 0.2$  associated with galaxies in the mean but that the Virgo Cluster in particular must have a much higher  $M/L_B$  value than the mean. The Numerical Action mean result for the field ( $M/L_B = 150M_\odot/L_\odot$ ) and the large mass for Virgo ( $M \sim 1.3 \times 10^{13} M_\odot$ ) are recorded in the right panel of Fig. 2.

As an aside, it should be noted that what is meant by the terms ‘group’ and ‘cluster’ are not well defined, other than that there is the inference that the structures are bound. In the case of the Local Group, it was discussed that there is a zero-velocity surface at  $\sim 1$  Mpc radius (Sandage 1986). This surface defines a bound domain and provides a logical limit to the group. However, the Local Group is certainly not virialized over this domain. At most, there may be limited quasi-virialized regimes within  $\sim 150$  kpc about each of the two dominant galaxies. By contrast, when we talk about the Virgo Cluster we certainly do not consider it to extend to the current zero-velocity surface which lies on the near side at about half the distance from us to the cluster core. Rather, a good working definition of the volume of the cluster is the domain within the first caustic, the outer limit of objects that have completed a single passage. The cluster is not virialized to this radius but the approach toward virialization will be greater within a cluster defined this way than in the Local Group analog.

The discussion to this point, involving the properties of groups and the inferences drawn from modeling of flow patterns in the Local Supercluster, has dealt with comparisons between intermediate and high density regimes. Attention will now turn to lower density environments.

## 5. THE LOW DENSITY REGIME

The algorithm for the selection of groups used by T87 contained luminosity. Could we loose real groups because their constituents are underluminous? We have just been arguing that groups with short crossing times and dominated by early type galaxies are environments that are

underluminous compared with the environments of groups with crossing times approaching a Hubble time and dominated by spirals and irregulars. Fortunately, no groups of the former type would have been missed in the construction of the group catalog because the E/S0 groups with short crossing times have considerably higher spatial densities than the spiral groups. Consequently they comfortably cross the luminosity density threshold set for the group catalog even though they turn out to be underluminous. In the years that have passed since the catalog was developed we have never become aware of a high spatial density but low luminosity group in the volume of our sample that escaped identification.

However we cannot be so sanguine in the limit of low spatial densities. Indeed, among the entities called ‘associations’ that came out of the T87 study there were some that look suspiciously like the entities identified as groups. The dimensions of these units are only several hundred kiloparsecs, like the groups. They can have *very low* velocity dispersions, comparable with the lowest values in the established groups. *Their members are all dwarfs.* They were not picked up in the groups analysis because they have very low luminosities. If they are bound groups then the associated  $M/L_B$  is much larger than is familiar to us from our experience with the intermediate regime spiral groups.

Our interest in these entities was rekindled by work from a very different direction. We were interested in possible environmental dependencies at the faint end of the luminosity function of galaxies. It seems that there are unexpectedly few dwarf galaxies compared with the expectations of the standard hierarchical model for galaxy formation (Klypin et al. 1999)(Moore et al. 1999). We suggested that the deficiency with respect to the standard model might be greater at lower densities (Tully et al. 2002), hereafter TSTV. There might be an expectation that there are many low mass dark matter halos floating about with little or no gas and stars. We speculated that there might be a possibility to identify the dynamical manifestations of such halos in a certain special environment. These low mass dark halos would not be of sufficient consequence to be noticed in our standard groups, even those as modest as the Local Group. At a mass and density regime well below that of the Local Group, according to the hypothesis that we are pursuing that low mass halos are voided of gas and stars, then there would be nothing to be seen. However, in the interval *between* the normal groups and putative much smaller structures it might be expected that *there are groups that are mostly, but not entirely dark.*

As discussed in TSTV, it occurred to us that the ‘mostly dark’ groups that could be anticipated from theoretical grounds might be found among the subset of associations in the T87 study with group-like dimensions and low velocity dispersions but high implied  $M/L_B$  values. We drew attention to four such groups thought to lie within 5 Mpc.

The key issue regarding these ‘groups of dwarfs’ that we identify is whether they are bound. *If they are bound then they must have high  $M/L_B$  values.* In order to illuminate this issue, we have been involved in programs to identify other potential group members and to get good distances to individual objects. These galaxies are all near enough

that they are easily resolved with Hubble Space Telescope (HST) and distances can be established from the luminosities of stars at the tip of the Red Giant Branch (Lee, Freedman, and Madore 1993), the ‘TRGB’ distance method. We first review the present status of these programs.

## 6. NEW DATA ON CANDIDATE GROUPS OF DWARFS

At the time of the paper by TSTV, good distances were only known for members of one of the four putative groups of dwarfs. Now there are reasonable distances from the TRGB method based on HST images for *most of the galaxies in all of the groups.* The new distances are reported in the following publications: Dohm-Palmer et al. (1998), Freedman et al. (2001), Karachentsev et al. (2002c), Karachentsev et al. (2003a), Karachentsev et al. (2003b), Maiz-Apellaniz et al. (2002), and Mendez et al. (2002).

The updated results are summarized in Table 2 for the four candidate groups of dwarfs and one additional comparison group. No weighting is applied in the calculation of the dimension, velocity, and mass parameters since it is assumed that the individual galaxies are inconsequential test particles in the potential of the group. The following information is provided in the table. (1) Group name from Tully (1988). (2) Prominent galaxy in group. (3) Number of candidate group members. (4) Mean group distance. (5) Inertial radius  $R_I^{3D} = (\sum_i^N r_i^2/N)^{1/2}$  where  $r_i$  is the 3-dimensional distance of a galaxy from the group centroid. (6) Radial velocity dispersion  $V_r = (\sum_i^N v_i^2/(N-1))^{1/2}$  where  $v_i$  is the radial velocity difference between a galaxy and the group mean (7) Blue Luminosity. (8) “Projected mass estimate”  $M_{pm} = \frac{f_{pm}^{3D}}{G(N-\alpha)} \sum_i^N r_i v_i^2$  (Heisler et al. 1985) where  $f_{pm}^{3D} = 5$  (TSTV) and  $\alpha = 1.5$ . (9) Virial mass estimate  $M_v = 3 \frac{(N-1)}{N} V_r^2 R_G / G$  where  $R_G = N / \sum_{pairs} (1/r_{ij})$  and  $r_{ij}$  is the separation between pairs in the group counted only once. The factor 3 gives the statistical conversion from the observed radial velocity to 3-dimensions. Radii are already provided in 3-dimensions because of the availability of distances. (10) Mass to light ratio based on the projected mass estimator. (11) Mass to light ratio based on the virial analysis. (12) Mass to light ratio given by TSTV. (13) Crossing time as a fraction of the Hubble time  $t_x H_0 = 38 R_I^{3D} / V_r$  where  $R_I^{3D}$  is in Mpc and  $V_r$  is in  $\text{km s}^{-1}$  and  $H_0 = 75 \text{ km s}^{-1} \text{ Mpc}^{-1}$ .

In TSTV, only the projected mass estimator of Heisler et al. (1985) was considered. Here we also provide the unweighted virial mass estimator. There can be circumstances with small numbers where the virial mass estimator gives ambiguous results; see the case of the NGC 3109 Group discussed below. However the use of the two mass estimators provides a better feel for the considerable uncertainties.

The  $M/L_B$  values determined by TSTV are carried for convenience into Table 2. It can be seen that  $M/L_B$  values have increased slightly overall with the current analysis. A principal cause of this small increase was a mistake in corrections to luminosities of galaxies in TSTV. In that paper the luminosities had corrections for obscuration based on the prescription by de Vaucouleurs et al. (1991). However, the obscuration in dwarf galaxies is sufficiently low as to be unmeasurable (Tully et al. 1998). In this paper,

no correction is made for obscuration within galaxies with  $M_B > -16$ . The result is that luminosities are systematically lowered and  $M/L_B$  values are increased. Corrections are made for obscuration due to lines of sight through our Galaxy (Schlegel, Finkbeiner, and Davis 1998). In any event, the luminosities of dwarf galaxies are often poorly known. Errors in the group luminosities of up to 30% are possible, but errors at this level do not bring the conclusions of this study into question. Here are comments on the situation in individual groups.

*14+12 = NGC 3109 Group:* The existence of this nearby entity as a distinct group was suggested by van den Bergh (1999). In our earlier analysis we entertained that GR8 = DDO 155 might be a member but this galaxy is significantly farther away than was assumed by TSTV, at 2.24 Mpc rather than 1.51 Mpc (Dohm-Palmer et al. 1998). This galaxy is also, by a substantial amount, the farthest removed from the other group candidates on the plane of the sky. Consequently, we eliminate this object from consideration as a group member. Moreover the object LSBC D634-03 is now revealed to be a background galaxy coincident with an HI high velocity cloud. The other 4 candidates are still considered at the distances given in TSTV. In the case of this group, the virial mass estimator is particularly untrustworthy because two of the candidates are very close neighbors; NGC 3109 and Antlia are separated by 29 kpc. Since  $R_G \sim 1/\sum(1/r_{ij})$ , the single pair dominates by an order of magnitude over the next pair in the calculation of the scale of the potential well. If the separation of this pair is arbitrarily set to 100 kpc, still smaller than any other separation in the group, then the virial mass estimate doubles. There is a chronic ambiguity in the virial mass estimator with small numbers and instances of close pairs. However, only this one group suffers this problem among the cases we are considering. Overall, the viability of the 14+12 candidate group remains as it was with the discussion by TSTV, with an implied  $M/L_B \sim 400$  if the entity is bound.

*14+8 = UGC 8760 Group:* Distance measurements have revealed that this group is much closer than the  $\sim 5$  Mpc that we expected. There are now TRGB distances for all the candidates, including a new and provisional one for UGC 8760 itself. Being closer, the linear separations are smaller than we appreciated. Also we have become aware of a fourth system, UGC 9240, which also is probably associated. The three well measured distances are very similar (UGC 8651 at 3.01 Mpc; UGC 8833 at 3.19 Mpc; UGC 9240 at 2.79 Mpc). The first two were associated with the group by TSTV and it is a powerful claim for the reality of the group that they both have unexpectedly low and similar distances. A nice test for the hypothesis being pursued is that the distance of UGC 8760 be also low and an HST observation returned as this paper goes to press reveals UGC 8760 to be at  $\sim 3.2$  Mpc. It is seen in Table 2 that the new  $M/L_B$  values are consistent between methods and considerably larger than found previously. The difference from the TSTV results is most marked in this case. Part of this increase is a direct consequence of the downward revision in distance;  $M/L_B$  is inversely dependent on distance. The other causes are the addition of the fourth candidate member and the changes to luminosities discussed above. A value  $M/L_B \sim 1000$  is required if the

entity is bound.

*14+19 = UGC 3974 Group:* All four candidate members now have TRGB distance measures and they all turn out to have distances similar to our expectation of  $\sim 5$  Mpc (UGC 3755 at 5.0 Mpc; UGC 3974 at 5.2 Mpc; UGC 4115 at 5.5 Mpc; KK98 65 at 4.5 Mpc). These galaxies are rather at the limit of the TRGB method with the HST WFPC detector in one orbit so the uncertainties are larger in these distances. Even so, contributions to the scale of the group from distances and projected separations are comparable. Again  $M/L_B$  values are larger than found before. The earlier result was based on the projected mass estimator with 2-D positions and particularly uncertain luminosities. The current analysis has revised luminosities and 3-D positions. Giving consideration to both mass estimators, the current information suggests  $M/L_B \sim 2000$  if the group is bound.

*17+6 = NGC 784 Group:* All 4 candidates have TRGB distances now although those for NGC 784 and UGC 1281 are unpublished and poor quality. The agreement is satisfactory and give a mean distance of 5.0 Mpc, as was initially anticipated. (UGC 1281 at 4.8 Mpc, NGC 784 at 4.6 Mpc, KK98 16 at 5.7 Mpc; KK98 17 at 5.0 Mpc). The factor 3 larger  $M/L_B$  than previously is attributable to the correction to luminosities and the distance differentials that reveal this group is extended more in the line-of-sight than in projection. If the group is bound then  $M/L_B \sim 1000$ .

*14+13 = Foreground Sculptor Group, a comparison case:* This structure was included in the discussion by TSTV. In the past, several of the galaxies have been considered as part of the Sculptor Group but we consider this historical group to consist of two distinct entities. We give attention to the nearer part. One good new candidate is added to the group specified by TSTV: ESO 294-010. All but the group's most luminous galaxy, NGC 55, have measured distances now (ESO 294-010 at 1.92 Mpc; NGC 300 at 2.00 Mpc; UGCA 438 at 2.23 Mpc; IC 5152 at 2.07 Mpc). Results are little different than previously. The mass estimates are as low as for any of the groups discussed above because of the very low velocity dispersion. However there are two moderate galaxies in the group so there is substantial luminosity. IC 5152 is removed by 770 kpc from the group centroid, mostly in projection, so the status of this object is in doubt. Whether or not it is included, if the entity is assumed to be bound then  $M/L_B \sim 17$ .

## 7. COMPARISON OF DWARF GROUP PROPERTIES

The candidate groups have mass estimates in the modest range  $1 - 9 \times 10^{11} M_\odot$ . Characteristic dimensions range  $290 \text{ kpc} < R_I < 540 \text{ kpc}$  with a mean of 420 kpc, typical of more familiar groups (T87). Velocity dispersions range from  $36 \text{ km s}^{-1}$  down to an incredibly low  $13 \text{ km s}^{-1}$  with a mean of  $22 \text{ km s}^{-1}$ . These values are all very low compared to familiar luminous groups and account for the low mass estimates. Luminosities are all in the decade  $1 - 10 \times 10^8 L_\odot$  except for the comparison case of the 14+13 or Foreground Sculptor Group which has almost an order of magnitude more luminosity than the most luminous of the others.

Crossing times as a fraction of the Hubble time are given in the last column of Table 2. Typically values are  $\sim 0.8H_0$ . Of course, the crossing times are long because

the velocity dispersions are so low. They are a sufficiently large fraction of the age of the Universe that one can worry that velocities are simply attributable to the expansion of the Universe; ie, that these are not bound groups. Only in the case of the tight 17+6 (NGC 784) Group is the crossing time substantially less than a Hubble time,  $H_0^{-1}$ . If IC 5152 is accepted as part of the 14+13 (Foreground Sculptor) Group then the crossing time for this group is 50% longer than  $H_0^{-1}$ , but this is the comparison case: a group with low  $M/L_B$ .

To this point there has been almost no discussion of uncertainties. First, it is to be emphasized that the measurement errors in the observed parameters are of almost no consequence. The radial velocities are obtained by observations of the 21cm line of HI and for these dwarfs are determined with an accuracy of  $\pm 5 \text{ km s}^{-1}$ . The distances are determined with the TRGB method. There might be a distance scale zero point issue at the level of 10% that would shift the entire sample in a similar fashion and not affect this discussion. Relatively, the distances should be accurate to 5% for galaxies within 3 Mpc. There is a degradation to 10 – 15% at 5 Mpc. However in none of the groups discussed here is the depth of the group dominant over the projected dimensions. Hence errors in measured dimensions do not make a significant contribution to uncertainties. The most poorly known direct observables are the luminosities. The global group luminosities attributable to the identified candidates can have errors as large as 30%. The luminosities come from heterogeneous sources, some with large errors. The situation could be improved with dedicated observations. Still, the real uncertainties lie elsewhere.

The greatest uncertainty of all is whether or not the groups are bound. Assuming for the moment that they are, then there are four dominant uncertainties in the calculation of a group mass: (a) small number statistics, (b) the statistics of velocity deprojection from one to three dimensions, (c) potentially poor coverage of the group gravitational well, and (d) the nature of the galaxy orbits. The first two of these problems lead to uncertainties that are statistical in nature. The groups under consideration have 4 or 5 candidate members each. The number of pairs grows as  $N(N-1)/2$  so each additional candidate gives a big improvement. As for the velocity deprojection problem, recall that mass calculation involves  $V^2$  and the deprojection correction is a factor 3. The latter two problems raise possibilities of systematic errors in the mass calculations. With regard to the question of coverage of the group potential well, one aspect is simply the limited coverage with only 4 or 5 test particles and another aspect is the uncertainty in the limits of the putative bounded regions. Do the candidates at larger radii represent those limits, or are they frequently beyond those limits and escaping? Finally, there is the nature of the galaxy orbits. Are they isotropized to a degree as would occur as a system approaches virialization or are they largely radial as would be expected of a group still in formation, with orbits dominated by infall? The alternatives have different implications for the projected velocities. Following the assumption of the virial theorem:  $2T/|W| = 1$ , where the kinetic energy per unit mass is  $T = \frac{3(N-1)}{2N} V_r^2$  and the potential energy per unit mass is  $W = -GM_v/R_G$  (see

section 6). The possibility of systematic departures from the virial condition was discussed in section 3. Both from analytic and N-body simulations (Merrall and Henriksen 2003) it is found that mean values of  $2T/|W|$  evolve from small values at turnaround to  $\sim 1$  at first collapse, to ratios up to 20% above unity, whence there is a slow approach to virialization from values above 1. There can be large excursions in individual cases. The results of this paper could require modification due to this probable systematic effect. Dense groups that are well advanced toward virialization will tend to have  $2T/|W|$  greater than unity by 0 – 20% so mass estimates will be above true values while groups that are still collapsing will tend to have  $2T/|W|$  less than unity by up to a factor 2 so mass estimates will be below true values.

Given the other large sources of errors, the uncertainty regarding the dynamical state is not dominant so the virial condition will be assumed. Mass estimates have been calculated two ways, following the discussion by Heisler et al. (1985). Except in the special case of the 14+12 (NGC 3109) Group that received discussion, the two mass estimates for a group differ from the mean by no more than 35%. If it is simply assumed that the group is bound then one gets a *lower mass limit* which is one-half the virial estimate. In the plots that will be shown further along, factor 3 uncertainties in mass have been assumed for groups with 4 candidates.

Even the very large uncertainties that have been discussed do not bring into question the fundamental claim being made pertaining to the low density regime. *If the candidate dwarf groups are bound then high  $M/L_B$  values are required for the groups.* We can think of two arguments that favor the point of view that the groups are bound. The first notes the continuity in properties with well established groups in terms of dimensions and velocity dispersions. These properties are illustrated in Figure 5. To a reasonable degree, the E/S0 dominated groups and spiral dominated groups separate on this plot. The early-type groups tend to be restricted spatially but can manifest large velocity dispersions while the late-type groups inevitably have modest velocity dispersions but can be dispersed spatially (there are a few groups with majority early types with the properties of the spiral groups). The candidate dwarf groups can be viewed as an extension of the distribution of the groups dominated by spirals. There is nothing to suggest from these parameters that characterize the dynamical state that the dwarf groups are other than a continuation of the family of bound groups to lower masses. It is only when attention is given to the luminosities of the systems that one appreciates that the situation is quite different from the familiar.

The second argument draws on the highly correlated nature of the distribution of dwarf galaxies. Within 5 Mpc, most known dwarfs are members of the few well established groups (14-7: CVn I Group; 14-10: M81 Group; 14-11: Maffei/IC 342 Group; 14-12: Local Group; 14-13: Sculptor Group; 14-15: Centaurus Group) and most of the rest are associated with a few relatively isolated bright galaxies or are members of the dwarf groups that have been identified. The current census of the sky for dwarf galaxies is mainly due to the hard work extracting candidates from the Second Palomar Observatory Sky



Survey in the northern sky and the ESO/SERC survey of the southern sky by Karachentseva and collaborators (Karachentseva and Karachentsev 1998), (Karachentseva et al. 1999), (Karachentsev et al. 2000), (Karachentseva and Karachentsev 2000), with HI follow up reported in Huchtmeier et al. (2001) and earlier papers. The HI Parkes All Sky Survey (HIPASS) is providing an independent search of the southern part of the sky (Barnes et al. 2001).

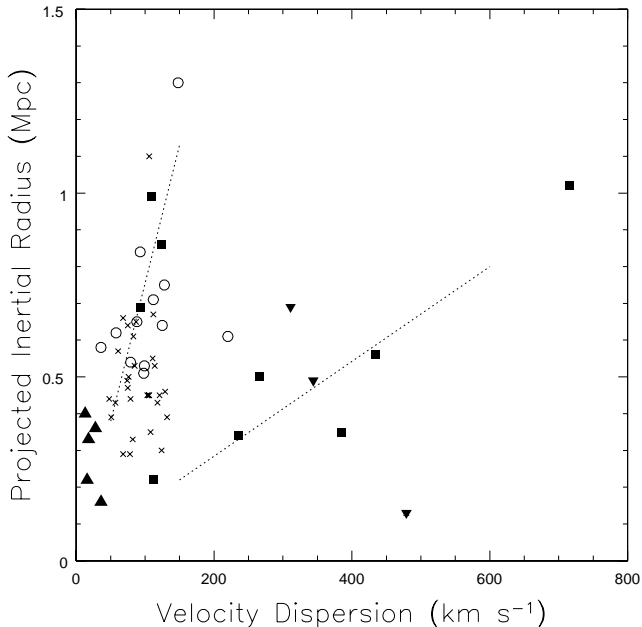


FIG. 5.— Group dimensions compared with group velocity dispersions. Groups dominated by early type galaxies: filled squares and inverted triangles. Groups dominated by late types: open circles. Small groups: crosses. Groups of dwarf galaxies (and 14+13 group): triangles. The separate trends of the early and late type groups are indicated by the dashed lines.

Karachentsev et al. (2003a) provide a tabulation of 156 galaxies, big and small, identified to exist between 1 and 5.5 Mpc of us (hence excludes the Local Group). Fully 101 of the objects are associated with the well established groups identified in the previous paragraph. Another 13 are associated with relatively isolated luminous galaxies and 6 are associated with somewhat more distant groups or are at very low galactic latitude. Then there are the 21 galaxies we associate with the groups of dwarfs or the comparison 14+13 (NGC 55) Group. That leaves only 15 low luminosity galaxies remaining through the rest of the volume. Several of these are in close proximity to one another.

The strong correlation in position of the nearby galaxies is illustrated in Figure 6. The top panel shows the two-point correlation function for all known galaxies at  $|b| > 28$  within 5 Mpc, excluding the Local Group within 1.1 Mpc. Good distances exist for a majority of these galaxies, and rough distances exist for the rest, so what is shown here is the three-dimensional two-point function. Normalization was achieved by comparison with 1000 monte carlo random distributions within the volume. The strong positive correlation at separations less than 1 Mpc is dominated by the contributions from the well known nearby galaxy groups.

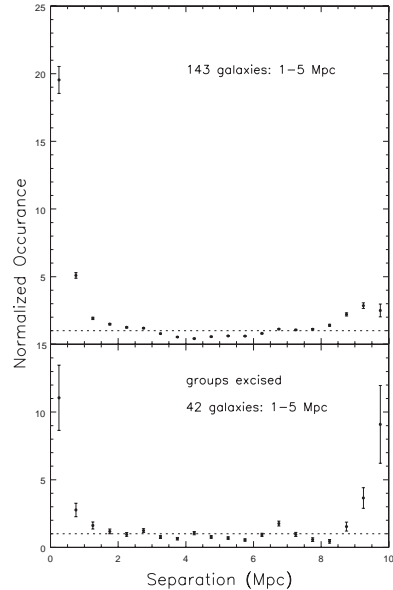


FIG. 6.— Two-point 3-dimension correlation functions. Top panel: correlation involving all 143 known galaxies within  $1.1 < d < 5$  Mpc and  $|b| > 28$ . Bottom panel: correlation with 42 galaxies after excising volumes containing five big groups.

The bottom panel in Fig. 6 examines the two-point correlation when contributions from the dominant groups have been excised. In this case, spheres of radius 1.4 Mpc have been defined centered on the 5 dominant nearby high latitude groups: those associated with M81, CVn I, Centaurus, Sculptor, and NGC 1313 (the Maffei Group lies at low latitude as does a majority of the Centaurus Group). The 80% of the volume that remains ( $220 \text{ Mpc}^3$ ) contains 30% of the original sample (42 galaxies). The Foreground Sculptor and three of four of our candidate dwarf groups are in the remaining volume, contributing 17 of the 42 galaxies (the 14+19 Group lies at low Galactic latitude; in fact the fussy  $|b| > 28$  limit was chosen to allow inclusion of the entire 17+6 Group).

It is seen that even when the historically known groups are eliminated there is still a strong correlation signal at separations less than 1 Mpc. The signal at separations less than 0.5 Mpc is 63% of the signal in the top panel. This signal is dominated by the correlations within the four low mass candidate groups.

The positive correlation signal at separations greater than 9 Mpc has an easy explanation. The monte carlo normalization assumes objects are distributed randomly throughout the available volume but in fact most nearby galaxies lie in the supergalactic equatorial plane. The signal at large separations comes from cross-correlations from opposite ends of the equatorial plane, between the 17+6 members and galaxies in the region of the Centaurus Group on the one hand and between galaxies in the vicinity of the Sculptor Group with those near CVn I and near Centaurus. In this small sample, only 3-4 galaxies in each of these regions is enough to create the spurious cross-correlation signal. The weaker signal at large separations in the top panel arises from the same source: the concentration of local galaxies to a plane.

The present analysis is preliminary because the census of dwarfs is still uncertain. It is still not clear that even

the high latitude sky has been uniformly surveyed. It is not clear how rapidly candidates are lost with Galactic latitude. HI signals for objects with velocities near zero can be lost in the confusion of Galactic emission. Our knowledge of the distances of candidates is improving rapidly with HST imaging but is still very incomplete. On the basis of present information the dwarf groups that have been identified are manifest enhancements over a random distribution. They correlate comparably well as the galaxies in previously established groups.

## 8. EVERYTHING TOGETHER

The small dimensions of the dwarf groups and the highly significant 2-point correlation signal on scales  $< 1$  Mpc suggest that the groups of dwarfs are bound. Given that proposition, we can add the information from the low density regime to the data from the intermediate and high density regime shown in Fig. 2. The combined data is seen in Figure 7. T87 groups of 2-4 members are added to provide information about the situation at low luminosities, though mass estimates are very uncertain for these entities. The four groups of dwarfs are plotted with error bars in mass. They lie at luminosities below  $10^9 L_\odot$  and well below the dotted  $M/L_B$  constant line. The comparison 14+13 (NGC 55) Group lies in the same mass range but at higher luminosity, well above the dotted line. The solid curve was fit to the ensemble of data. The curve corresponds to the expression:

$$L_B = \phi M^\gamma e^{-M^\dagger/M} \quad (2)$$

This equation relates luminosity and mass with 3 constraints: a logarithmic slope at the high mass end,  $\gamma$ , a low mass exponential cutoff set by  $M^\dagger$ , and a normalization,  $\phi$ . The curve was fit by minimizing a  $\chi^2$  with uncertainties taken in mass only:

$$\chi^2 = \sum_i^N \left( \frac{\log M_i - \log M_{fit}}{\log \sigma} \right)^2 \quad (3)$$

Here,  $M_{fit}$  is the mass in the relationship described by eq. (2) at the luminosity  $L_i$  of group  $i$ , with measured mass  $M_i$ . The  $\chi^2$  normalization is given the dependence on the number of group members  $N$  according to the formulation  $\log \sigma = A/N^{0.75}$ . A weighting that favors groups with large  $N$  more than the statistical  $N^{-0.5}$  is justified by the expected better approximation to a virialized state for the larger groups and to compensate for the small numbers of large  $N$  systems. The absolute normalization of the  $\chi^2$  evaluator is arbitrary: we simply search for the lowest value. We set  $A = 2$  for the traditional groups and  $A = 1$  for the groups of dwarfs; ie, give double weight to the groups of dwarfs because they are drawn from a restricted region and are few in number.

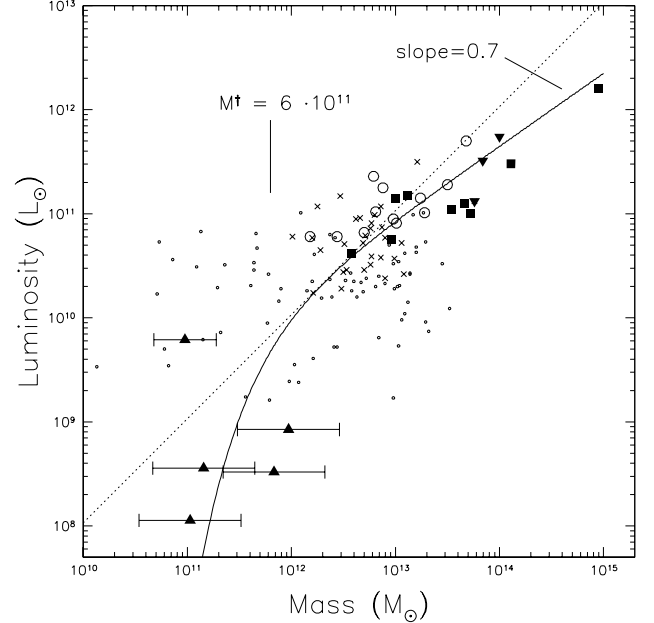


FIG. 7.— Mass vs. light for groups over the full range of density regimes. The data for the higher density regimes are the same as seen on the right panel of Fig. 2 with the addition of the small open circles which represent groups with 2–4 identified members. The 5 groups that explore the low density regime are plotted with error bars. The  $M/L_B = 94$  dotted line is carried over from Fig. 2. The solid line is the fit described in the text with a high mass slope of  $\gamma = 0.7$  and an exponential fall off at masses less than  $M^\dagger = 6 \times 10^{11} M_\odot$ .

The curve superimposed on the data in Fig. 7 has a slope at the high mass end of  $\gamma = 0.70$ . It can be appreciated that taking errors only in mass leads to a steeper slope than if errors are distributed into luminosity. At the low mass end the curve demonstrates an exponential cutoff characterized by  $M^\dagger = 6 \times 10^{11} M_\odot$ . The normal luminous groups with 5 or more members only provide information at masses  $> 10^{12} M_\odot$ . Groups of 2–4 members provide information at lower luminosities and masses but at the cost of large uncertainties in mass. The evidence for the cutoff comes from the four candidate dwarf groups. In the absence of the dwarf groups we might be left to suppose that there is simply a lower limit to the mass range of groups. However, from Fig. 7 we instead infer that smaller mass groups do exist but groups are not manifested by the light of stars at very low masses. The break is more dramatically represented in Figure 8. This plot shows the same data but the vertical axis gives the departure from a  $45^\circ$  line in the previous plot. Large errors in masses in small groups create diagonal scatter in this plot. The inference we draw from the Foreground Sculptor Group, with very low  $M_B/L$ , is that there is tremendous real scatter in the baryon content of halos in the proximity of the mass cutoff.

Interestingly, both Marinoni and Hudson (2002) and van den Bosch, Mo, and Yang (2003) have deduced a similar dependence between mass and light from observations of the luminosity function of galaxies derived from redshift surveys and the assumption that the underlying halo mass function follows the modified Press-Schechter description of Sheth and Tormen (1999). The deduction follows from the observation that, compared with the mass function, the luminosity function is shallower at the faint end and

cuts off more abruptly at the bright end, implying  $M/L$  increases at the two extremes relative to the intermediate range.

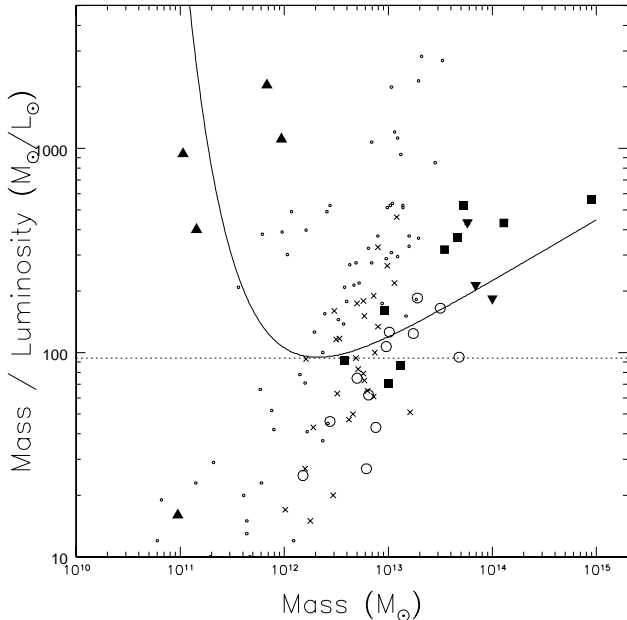


FIG. 8.— Mass to light ratio vs. mass over the full range of density regimes. The data are the same as in Fig. 7. The solid curve and dotted line are transpositions of the curve and line in Fig. 7.

To conclude, we take a look at the mass function in the volume with  $|b| > 30$  and a distance limit of  $25h_{75}^{-1}$  Mpc (distances from a numerical action velocity field model) and the fraction of the total mass lying in specific environments. This information is summarized in Figure 9. The mass function incorporates all the groups involved in the earlier discussion, plus contributions from galaxies that lie outside any of these groups. We have no information on the extended mass around individual galaxies but for the purpose of constructing this mass function it is assumed that  $M/L_B^{single} = 100M_{\odot}/L_{\odot}$ . The contribution of the individual galaxies by number is given by the figures in brackets in Fig. 9. It is seen that the individual galaxies only become dominant in their contribution below  $10^{12}M_{\odot}$  and with our  $M/L_B$  assumption for the individual galaxies their contribution to the overall mass budget is small.

The mass function shown in Fig. 9 becomes incomplete below  $10^{12}M_{\odot}$ . The error bars only reflect the statistical uncertainty associated with the observed contributions. To get an estimate of the contribution to the total mass budget of low mass groups we consider the restricted volume within 5 Mpc. In this volume there are 5 groups of luminous galaxies, excluding the low latitude 14-11 (Maffei/IC 342) Group, and these groups cumulatively contain about  $12 \times 10^{12}M_{\odot}$ . Three high latitude luminous galaxies unassociated with significant groups (NGC 1313, NGC 3621, and NGC 6503), if assumed to have an associated  $M/L_B = 100$ , would contain about  $2 \times 10^{12}M_{\odot}$  in their vicinity. The five low mass groups discussed here would cumulatively contain about  $2.0 \times 10^{12}M_{\odot}$ . Roughly 3/4 of the mass related to observable galaxies within 5 Mpc would lie in the major groups, almost 90% would be associated in some way with luminous galaxies, and only about 12%

would be in the regions of the groups of dwarfs. Although the number of groups associated with low mass halos are comparable to the number of familiar groups in the local region, they contribute only a small fraction of the mass. Hence the inventory of the mass of the Universe tied up in bound structures represented by Fig. 9 is unlikely to be seriously in error at the low mass end.

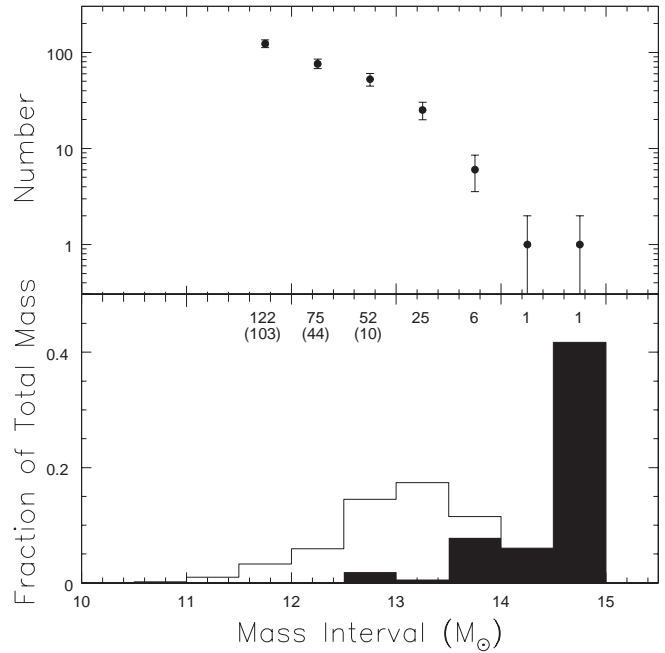


FIG. 9.— *Top panel:* Observed mass function in the volume within  $25h_{75}^{-1}$  Mpc and  $|b| > 30$ . The numbers of objects in each bin are given along the top of the lower panel. In brackets are the numbers of individual galaxies; ie, galaxies outside of groups. *Lower panel:* Fraction of the total mass associated with the mass function in half-dec bins. The mass associated with the groups of predominantly early types is indicated by the filled histograms. The open histograms correspond to the mass found in the groups with predominantly late types.

The histogram of mass fractions by mass interval seen in Fig. 9 can be summarized as follows. Fully 40% of the mass in this local volume is in the single object, the Virgo Cluster (clearly, the high mass end of the mass function is poorly determined in such a restricted volume). The groups that have short crossing times and are dominated by E/S0/Sa galaxies (including Virgo) contain 60% of the mass. Looking at groups of all types, 90% of the mass is in groups with  $\log M > 12.5$ . The luminous groups within 5 Mpc all lie essentially within the mass bin  $12.0 < \log M < 12.5$ , on the tail of the histogram seen in Fig. 9. Yet even with respect to such groups, the low mass groups within 5 Mpc make only a minor contribution to the mass budget. It can be concluded that they do not contain an important fraction of the mass of the Universe.

## 9. SUMMARY

There is surprisingly strong evidence for variations in the relationship between blue light and mass as a function of environment. On the scale of groups, the lowest  $M/L_B$  values are found on mass scales of  $10^{12} - 10^{13}M_{\odot}$  where typical values are  $M/L_B \sim 90M_{\odot}/L_{\odot}$ . Groups in this mass range are almost always composed of late type galaxies with ongoing star formation. Groups with higher mass

produce less blue light. The trend is enhanced by the local density as identified by the crossing time. High density regions, those with short crossing times, are darker. The morphology of the group members is highly correlated with these trends: groups with predominantly E/S0/Sa systems have short crossing times and large  $M/L_B$ . This pattern is consistent with a picture in which dense regions formed earlier and today star formation is largely exhausted in these places. The stellar populations are fainter and redder. Possibly in these environments there have been multiple collisions between galaxies that have scattered many stars into the intracluster environment where their light goes undetected in our light inventory. Then it is certainly known that the dense environments of E/S0 groups and clusters glow with thermal X-ray emission, to the degree that most of the baryons in these environments are in the hot intracluster gas and not in stars. Together, these astrophysical processes could explain the observed factor of 7 increase in  $M/L_B$  in proceeding from spiral dominated groups in the mass range  $10^{12} - 10^{13} M_\odot$  to E/S0 dominated groups in the mass range  $10^{14} - 10^{15} M_\odot$ .

At the other end of the mass spectrum, below  $10^{12} M_\odot$ , there is a cutoff in the visible manifestations of groups. One unlikely possibility is that there simply are few groups with less mass than  $10^{12} M_\odot$ . A more likely possibility is that group halos of lower mass exist but are difficult to identify because of a deficiency of light. We have presented evidence that such low mass groups might be common. The number of such groups that can be identified within 5 Mpc are comparable to the number of luminous groups. The deficiency of light is very great in these cases, assuming that the groups are bound. Groups in the mass range  $10^{11} - 10^{12} M_\odot$  can have  $M/L_B$  values 5 to 20 times higher than the groups of spiral galaxies in the range

$10^{12} - 10^{13} M_\odot$ . The possibility is open that there may be halos in the dwarf group mass range and lower that are totally invisible.

As an aside, if the hypothesis of this paper is correct that groups of dwarfs are bound then the two decade old controversy between the alternatives of dark matter versus non-Newtonian gravity (Milgrom 1983) is definitively resolved. It is implausible that the groups of dwarfs are bound by stars or gas. The relationship between the observable constituents and the gravitational field is quite unlike that of more luminous groups.

The transform between light and mass is being shown to be complex. Of particular cosmological importance is the sharp trend toward darkness at high mass. The Virgo Cluster has 40% of the mass attributed to groups in the volume of our study but it only contributes 15% of the blue light. The rich clusters have a dynamic importance much greater than would be expected from their light. By contrast, though there is evidence that low mass groups may be rendered almost or completely invisible, their cumulative contribution to the clustered mass of the Universe seems to be small. To the limit that it can be traced, the mass function is too flat for low mass structures to make a substantial contribution to the inventory of mass.

The work over the years involving the Numerical Action modeling has involved a happy collaboration with Jim Peebles and, especially, Ed Shaya. My principal collaborator on work at the faint end of the galaxy luminosity function is Neil Trentham. Jose Pacheco has provided valuable insight regarding the dynamic state of unrelaxed structures. This research is being supported by JPL Contract 1243647 and STScI awards HST-GO-09162 and HST-GO-10210.

## REFERENCES

- Barnes, D.G., Staveley-Smith, L., & de Blok, W.J. 2001, MNRAS, 322, 486
- Barnes, J. 1985, MNRAS, 215, 517
- Blanton, M., Cen, R., Ostriker, J.P., & Strauss, M.A. 1999, ApJ, 522, 590
- de Vaucouleurs, G. et al. 1991. Third Reference Catalogue of Bright Galaxies, (Springer-Verlag)
- Dohm-Palmer, R.C. et al. 1998, AJ, 116, 1227
- Evans, N.W., Wilkinson, M.I., Guhathakurta, G., Grebel, E.K., & Vogt, S.S. 2000, ApJ, 540, L9
- Freedman, W.L. et al. 2001, ApJ, 553, 47
- Funato, Y., Makino, J., & Ebisuzaki, T. 1992, PASJ, 44, 291
- Gould, A. 1993, ApJ, 403, 37
- Heisler, J., Tremaine, S., & Bahcall, J.N. 1985, ApJ, 298, 8
- Huchtmeier, W.K., Karachentsev, I., & Karachentseva, V.E. 2001, A&A, 377, 801
- Ibata, R., Chapman, S., Ferguson, A.M.N., Irwin, M., Lewis, G., & McConnachie, A. 2004, MNRAS, (astro-ph/0403068)
- Lynden-Bell, D. 1967, MNRAS, 136, 101
- Kahn, F.D., & Woltjer, L. 1959, ApJ, 130, 705
- Kaiser, N. 1984, ApJ, 284, L9
- Karachentsev, I. 2004, AJ, to be submitted
- Karachentsev, I., Karachentseva, V.E., Suchkov, A.A., & Grebel, E.K. 2000, A&AS, 145, 415
- Karachentsev, I., Dolphin, A.E., Geisler, D. et al. 2002a, A&A, 383, 125
- Karachentsev, I., Sharina, M.E., Dolphin, A.E. et al. 2002b, A&A, 385, 21
- Karachentsev, I., Sharina, M.E., Makarov, D.E. et al. 2002c, A&A, 389, 812
- Karachentsev, I., Makarov, D.I., et al. 2003a, A&A, 398, 479
- Karachentsev, I., Sharina, M.E., et al. 2003b, A&A, 408, 111
- Karachentseva, V.E., & Karachentsev, I. 1998, A&AS, 127, 409
- Karachentseva, V.E., & Karachentsev, I. 2000, A&AS, 146, 35
- Karachentseva, V.E., Karachentsev, I., & Richter, G.M. 1999, A&AS, 135, 221
- Klypin, A., Kratsov, A.V., Valenzuela, O., & Prada, F. 1999, ApJ, 522, 82
- Lee, M.G., Freedman, W.L., & Madore, B.F. 1993, ApJ, 417, 417
- Maiz-Apellaniz, J., Cieza, L., & MacKenty, J.W. 2002, AJ, 123, 1307
- Marinoni, C. & Hudson, M.J. 2002, ApJ, 569, 101
- Mendez, B., Davis, M., Moustakas, J., Newman, J., Madore, B.F., & Freedman, W.L. 2002, AJ, 124, 213
- Merrall, T.E.C., & Henriksen, R.N. 2003, ApJ, 595, 43
- Milgrom, M. 1983, ApJ, 270, 371
- Moore, B., Ghigna, S., Governato, F., Lake, G., Quinn, T., Stadel, J., & Tozzi, P. 1999, ApJ, 524, L19
- Ostriker, J.P., Nagamine, K., Cen, R., Fukugita, M. 2003, ApJ, (astro-ph/0305203)
- Peebles, P.J.E. 1995, ApJ, 449, 52
- Quintana, H., Fouqué, P., & Way, M.J. 1994, A&A, 282, 722
- Sandage, A. 1986, ApJ, 307, 1
- Schlegel, D.J., Finkbeiner, D.P., & Davis, M. 1998, ApJ, 500, 525
- Shaya, E.J., Peebles, P.J.E., & Tully, R.B. 1995, ApJ, 454, 15
- Sheth, R.K. & Tormen, G. 1999, MNRAS, 308, 119
- Somerville, R.S., Lemson, G., Sigad, Y., Dekel, A., Kauffmann, G., White, S.D.M. 2001, MNRAS, 320, 289
- Tonry, J.M. & Davis, M. 1981, ApJ, 246, 680
- Trentham, N. & Tully, R.B. 2002, MNRAS, 335, 712
- Tully, R.B. 1987, ApJ, 321, 280 [T87]
- Tully, R.B. 1988, Nearby Galaxies Catalog, Cambridge University Press
- Tully, R.B., Pierce, M.J., Huang, J.S., Saunders, W., Verheijen, M.A.W., & Witchalls, P.L. 1998, AJ, 115, 2264
- Tully, R.B. & Shaya, E.J. 1984, ApJ, 281, 31
- Tully, R.B. & Shaya, E.J. 1998, Proc. Evolution of Large Scale Structure, eds. R.K. Sheth & A.J. Banday (astro-ph/9810298)
- Tully, R.B., Somerville, R.S., Trentham, N., & Verheijen, M.A.W. 2002, ApJ, 569, 573 [TSTV]

van den Bosch, F.C., Mo, H.J., & Yang, X. 2003, MNRAS, 345, 923

van den Bergh, S. 1999, ApJ, 517, L97

TABLE 1  
 PROPERTIES OF GROUPS FROM T87.

Group	$N_{gal}$	% Early	Dist. (Mpc)	$V_g$ ( $\text{km s}^{-1}$ )	$V_r$ ( $\text{km s}^{-1}$ )	$R_I$ (Mpc)	$t_x H_0$	$\log L_B$ ( $L_\odot$ )	$\log M_v$ ( $M_\odot$ )	$M_v/L$ ( $M_\odot/L_\odot$ )
11-01	174	61	16.8	1042	715	1.02	0.08	12.20	14.95	562
11-04	7		13.8	1576	124	0.30	0.13	10.59	12.77	151
11-10	9	17	23.9	1221	79	0.54	0.36	11.36	12.79	27
11-14	5		19.2	838	106	1.10	0.55	11.50	13.21	51
12-01	57	22	17.2	967	148	1.30	0.47	11.70	13.68	95
12-03	9	22	22.9	1352	112	0.71	0.34	11.01	13.28	185
12-05	6		23.0	1384	83	0.61	0.39	10.95	12.62	47
12-06	9	29	20.1	1020	125	0.64	0.27	10.91	13.01	126
14-01	25	52	9.7	911	266	0.50	0.10	11.00	13.72	523
14-04	22	14	7.6	596	58	0.62	0.56	10.78	12.44	46
14-05	8		7.3	571	129	0.46	0.19	10.77	12.90	134
14-06	5		7.8	698	78	0.29	0.20	10.44	12.50	116
14-07	22		3.5	309	51	0.39	0.41	10.24	12.21	93
14-09	9		5.0	367	82	0.33	0.21	10.46	12.53	117
14-10	12		3.3	242	108	0.35	0.17	10.46	12.70	174
14-11	8		3.0	188	75	0.47	0.33	11.17	12.47	20
14-12	10		0.0	-18	57	0.43	0.40	10.78	12.01	17
14-13	11		2.1	197	118	0.43	0.19	10.38	12.90	28
14-15	12		4.3	304	68	0.66	0.52	10.96	12.66	50
15-01	9	88	7.2	626	112	0.22	0.10	10.62	12.58	92
17-01	13	9	10.0	752	36	0.58	0.85	10.78	12.18	25
17-04	6		9.8	813	114	0.53	0.25	10.57	12.99	266
19-01	8		10.6	735	87	0.65	0.39	10.86	12.76	79
21-01	11	36	22.9	1087	220	0.61	0.15	11.28	13.50	165
21-03	10	0	20.9	1009	98	0.51	0.28	10.82	12.70	75
21-06	12	55	22.3	1207	124	0.86	0.37	11.15	13.00	71
21-10	5		20.1	1082	61	0.57	0.49	10.77	12.20	27
21-12	10	30	24.5	1453	88	0.65	0.39	11.02	12.81	62
41-07	5		24.0	1219	132	0.39	0.16	11.07	12.86	61
43-01	13	11	19.2	970	128	0.75	0.31	11.15	13.24	124
44-01	7		15.9	922	76	0.50	0.35	10.79	12.71	83
51-01	31	90	16.9	1344	434	0.56	0.07	11.48	14.11	431
51-04	17	62	17.9	1427	110	0.99	0.48	11.18	13.12	87
51-05	6		19.9	1601	85	0.53	0.33	10.87	12.87	100
51-07	6		20.2	1626	112	0.67	0.32	10.99	12.80	65
51-08	23	94	25.0	1552	385	0.35	0.06	11.10	13.66	364
52-01	11	29	17.1	1405	99	0.53	0.28	10.95	12.98	107
52-02	8		13.8	1125	75	0.64	0.45	10.91	12.77	73
52-03	5		19.1	1567	105	0.45	0.23	10.58	12.86	190
52-06	6		18.6	1531	79	0.44	0.29	10.65	12.28	43
52-07	6		23.7	1954	48	0.44	0.49	11.07	12.25	15
53-01	13	82	13.4	1006	236	0.34	0.08	11.04	13.54	319
53-03	5		15.0	1109	121	0.45	0.20	10.42	13.08	460
53-07	15	50	10.8	833	93	0.69	0.39	10.75	12.96	161
53-10	5		11.4	831	103	0.45	0.23	10.51	12.76	179
54-01	7		13.7	802	111	0.55	0.26	10.72	13.06	219
54-03	5		8.4	519	68	0.29	0.22	10.28	12.48	160
61-11	6		23.2	1852	106	0.45	0.22	10.71	12.51	63
61-16	12	40	19.3	1572	93	0.84	0.48	11.25	12.88	43
65-01	6		14.6	1132	74	0.49	0.35	10.72	12.69	94
11-24 <sup>a</sup>	12	92	35.2	2148	311	0.69	0.12	11.74	14.00	184
31-02 <sup>a</sup>	10	70	37.5	2188	479	0.13	0.01	11.12	13.76	434
41-01 <sup>a</sup>	11	73	28.4	1807	344	0.49	0.08	11.51	13.84	214

<sup>a</sup>Early type group beyond 25 Mpc

TABLE 2  
 PROPERTIES OF GROUPS OF DWARF GALAXIES.

Group	Principal Galaxy	No.	Dist. (Mpc)	$R_I^{3D}$ (Mpc)	$V_r$ (km s $^{-1}$ )	$L_B$ ( $10^8 L_\odot$ )	$M_{pm}$ ( $10^{11} M_\odot$ )	$M_v$ ( $10^{11} M_\odot$ )	$M_{pm}/L$ ( $M_\odot/L_\odot$ )	$M_v/L$ ( $M_\odot/L_\odot$ )	$M/L_B^{old}$ ( $M_\odot/L_\odot$ )	$t_x H_0$
14+12	NGC 3109	4	1.4	0.34	18	3.6	1.4	0.6 <sup>a</sup>	400	200 <sup>a</sup>	1220	0.83
14 +8	UGC 8760	4	3.0	0.29	16	1.1	1.0	1.2	860	1030	250	0.76
14+19	UGC 3974	4	5.0	0.54	28	3.3	5.1	8.5	1520	2560	1060	0.84
17 +6	NGC 784	4	5.0	0.45	36	8.5	8.3	10.5	980	1240	330	0.54
14+13	NGC 55	4	2.1	0.30	15	57.6	0.9	1.1	16	18	13	0.85
		5 <sup>b</sup>		0.47	13	61.5	0.8	1.1	14	18		1.5

<sup>a</sup>Virial mass estimate biased low: close pair

<sup>b</sup>Including IC 5152 in group